

## ORIGINAL ARTICLE

# A design of impedance transformer with tunable center frequencies using filter synthesis approach

Girdhari Chaudhary  | Yongchae Jeong 

Division of Electronics and Information Engineering, IT Convergence Research Center, Jeonbuk National University, Jollabuk-do, Republic of Korea

**Correspondence**

Yongchae Jeong, Division of Electronics and Information Engineering, IT Convergence Research Center, Jeonbuk National University, Jollabuk-do 54896, Republic of Korea.

Email: [ycjeong@jbnu.ac.kr](mailto:ycjeong@jbnu.ac.kr)

**Funding information**

National Research Foundation of Korea (NRF) Grant Funded by Korean Government (MSIT), Grant/Award Number: 2020R1A2C2012057; Basic Science Research Program through NRF Funded by Ministry of Education, Grant/Award Number: 2019R1A6A1A09031717; Research Base Construction Fund Support Program Funded by Jeonbuk National University in 2021

**Abstract**

Microwave impedance transformer (IT) with center frequency tunable capability is one of great research issue for better utilization of frequency spectrum resources and system miniaturization of next generation wireless communication systems. This article presents a filter synthesis approach for designing IT with center frequency tunable capability using single dc-bias controlled tunable resonators. The proposed IT provides bandpass filtering response and is designed by properly coupling quarter-wave tunable resonators with alternate *J*- and *K*-inverters. The *J*-inverters are realized using a parallel-coupled line, whereas *K*-inverter is implemented with T-type short-circuited TL. Using filter theory, analytical design equations are derived to calculate the circuit parameters. The center frequency of the proposed IT is tuned over a wide frequency tuning range (FTR) by changing the varactor diode capacitance of quarter-wave resonators. For experimental demonstration, a prototype of 25-to-50  $\Omega$  IT is designed, simulated, and measured. The measured results confirmed that the center frequency of the proposed IT is tuned from 2.05 to 2.91 GHz (860 MHz or 34.68% FTR) with an insertion loss variation of 2.57 to 1.76 dB.

**KEYWORDS**

bandpass filter response, frequency tunable, impedance transformer, quarter-wave transmission line resonator

## 1 | INTRODUCTION

Impedance transformer (IT), which convert certain impedance into another one; is one of key components in radio frequency and microwave systems. These ITs are widely used for power dividers/combiner, power amplifiers, and antenna feeding networks.<sup>1–7</sup> In general, IT can be easily realized using quarter-wave ( $\lambda_g/4$ ) transmission line (TL), however, it cannot provide bandpass filtering response. More recently, various designs of filtering ITs have been presented with different topologies including parallel coupled lines with shunt open/short stubs, multi-section parallel coupled lines, and stepped impedance resonators.<sup>8–11</sup> Likewise, wideband filtering ITs with out-

of-band suppression are presented in References 12,13, using coupled line and shunt half-wavelength TL. In References 14,15, ITs with enhanced impedance transforming ratio and wide out-of-band suppression are demonstrated. Using multi-section coupled line and modified coupled line, the wideband ITs are presented in References 16–18. In References 19–21, ITs with extremely low or high impedance transforming are presented. More recently, the multi-band ITs are presented in References 22–23. In Reference 24, tunable IT is demonstrated at fixed center frequency using split strip lines. Despite significant research, conventional ITs are designed for fixed center frequency and none of the previously reported ITs can provide the center frequency tunability.

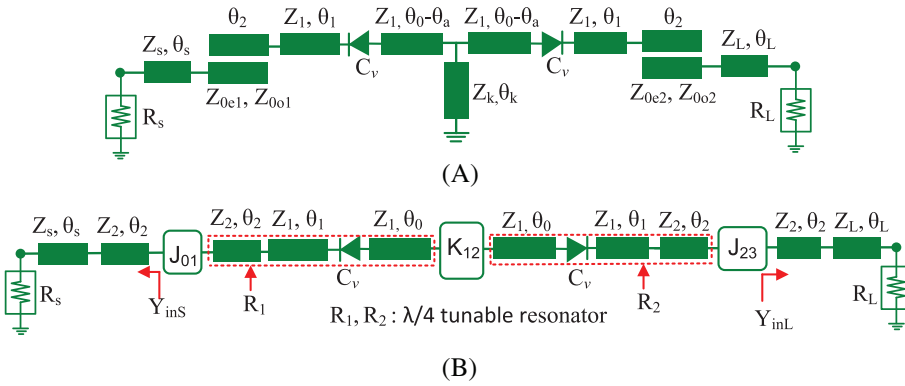


FIGURE 1 (A) Proposed structure of impedance transformer with tunable center frequency and (B) equivalent circuit of proposed impedance transformer

Simultaneous impedance transformation and center frequency tunable capability of IT are of great interest to future wireless communication for better utilization of limited frequency spectrum resources and system miniaturization.

In this article, we present a filter synthesis approach to design filtering IT with center frequency tunability capability over a wide frequency tuning range (FTR) using  $\lambda_g/4$  TL resonators. The frequency tunability can be achieved by tuning the bias voltage of a varactor diode. We derive general design equations for designing IT with center frequency tunability by using filter theory.

## 2 | ANALYTICAL ANALYSIS

### 2.1 | Proposed structure of impedance transformer

Figure 1A shows the proposed structure of the IT with tunable center frequency. The source and load impedances are terminated with  $R_s$  and  $R_L$ , respectively. The proposed IT consists of source/load connecting transmission lines (TLs), parallel-coupled lines, tunable resonators, and T-type TLs. The TL with  $Z_s = 1/Y_s$  and  $\theta_s$  and the TL with  $Z_L = 1/Y_L$  and  $\theta_L$  are connected at source and load, respectively. The tunable resonators ( $R_1, R_2$ ) are coupled to source/load connecting TLs through coupled lines. The equivalent circuit of the proposed IT is shown in Figure 1B. The parallel-coupled lines are equivalent to  $J$ -inverters, whereas the T-type TLs are equivalent to  $K$ -inverters. Using filter theory, the values of  $J$ - and  $K$ -inverters are determined<sup>25</sup> as (1).

$$J_{01} = \sqrt{\frac{\text{Re}(Y_{inS})\Delta b}{g_0 g_1}} \quad (1a)$$

$$K_{12} = \frac{\Delta x}{\sqrt{g_1 g_2}} \quad (1b)$$

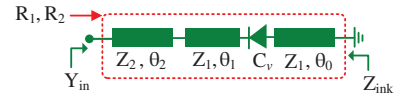


FIGURE 2 The proposed structure of a tunable quarter-wave resonator

$$J_{23} = \sqrt{\frac{\text{Re}(Y_{inL})\Delta b}{g_2 g_3}} \quad (1c)$$

where  $g_i$  ( $i = 0, 1, 2, 3$ ),  $\Delta$ ,  $b$ , and  $x$  are low-pass prototype-element values, fractional bandwidth, susceptance slope parameter and reactance slope parameter of tunable resonator, respectively. Similarly,  $\text{Re}(Y_{inS})$  and  $\text{Re}(Y_{inL})$  are the real part of input impedance looking at the first and last inverter as shown in Figure 1B, respectively.

### 2.2 | Resonant frequency and slope parameter of resonator

Figure 2 shows the proposed structure of a tunable  $\lambda_g/4$  resonator. The resonator consists of three TLs with characteristic impedance and electrical lengths of  $Z_1, Z_2, \theta_0, \theta_1, \theta_2$ , and a varactor diode capacitance  $C_v$ . The input admittance looking toward short-circuit TL is given as (2).

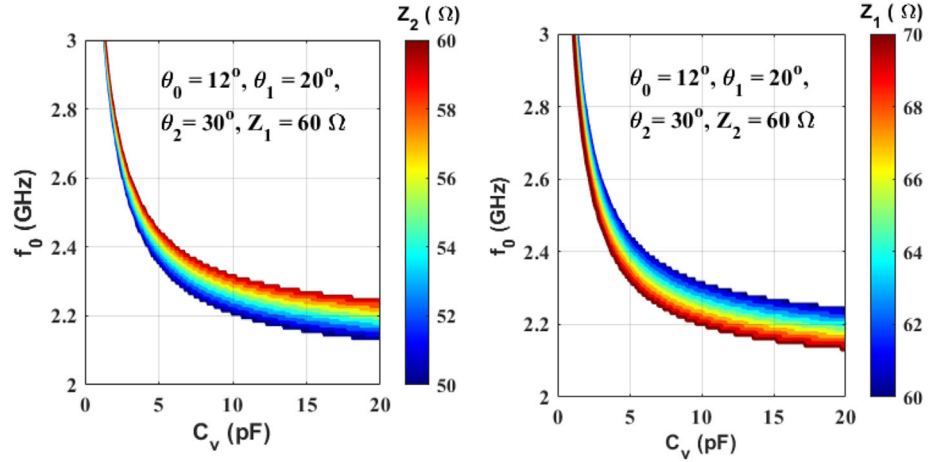
$$Y_{in} = jY_2 \frac{Y_A + Y_2 \tan \theta_2}{Y_2 - Y_A \tan \theta_2} = jB, \quad (2)$$

where

$$Y_A = Y_1 \frac{Y_B + Y_1 \tan \theta_1}{Y_1 - Y_B \tan \theta_1}, Y_B = \frac{2\pi f C_v Y_1 \cot \theta_0}{Y_1 \cot \theta_0 - 2\pi f C_v}, Y_1 = \frac{1}{Z_1}, Y_2 = \frac{1}{Z_2} \quad (3)$$

Similarly, the input impedance toward open circuited TL shown in Figure 2, is given as (4).

**FIGURE 3** Resonant frequency of the proposed resonator according to  $C_v$ ,  $Z_1$ , and  $Z_2$ . Electrical lengths of TLs ( $\theta_0$ ,  $\theta_1$ ,  $\theta_2$ ) are defined at 1.50 GHz. Color bar represents value of  $Z_1$  and  $Z_2$



$$Z_{ink} = jZ_1 \frac{Z_M + Z_1 \tan\theta_0}{Z_1 - Z_M \tan\theta_0} = jX, \quad (4)$$

where

$$Z_M = Z_1 \frac{Z_1 \tan\theta_1 - Z_2 \cot\theta_2}{Z_1 + Z_2 \cot\theta_2 \tan\theta_1} - \frac{1}{2\pi f C_v}. \quad (5)$$

The resonant frequency ( $f_0$ ) can be solved by setting  $B = \text{im}(Y_{in}) = 0$  or  $X = \text{im}(Z_{ink}) = 0$ . Similarly, the susceptance slope parameter ( $b$ ) and reactance slope parameter ( $x$ ) of the resonator at resonant frequency  $f_0$  can be found as (6).

$$b = \left. \frac{f_0 dB}{2 df} \right|_{f=f_0} \quad (6a)$$

$$x = \left. \frac{f_0 dX}{2 df} \right|_{f=f_0} \quad (6b)$$

Figure 3 shows the calculated resonant frequencies of the proposed resonator. The resonant frequency decreases as  $C_v$  increases. From this figure, we also note that resonant frequency is high when  $Z_1$  is low and  $Z_2$  is high for the same  $C_v$ .

### 2.3 | Analysis of source and load connecting transmission lines

The source/load connecting TLs ( $Z_S$ ,  $\theta_S$ , and  $Z_L$ ,  $\theta_L$ ) used to match source/load impedances to another real impedance at the first and last inverters. Using Figure 1B, input admittances ( $Y_{ins}$ ) at first  $J$ -inverter looking toward source terminated impedance ( $R_S$ ) is given as (7) assuming the impedance transforming ratio  $r = R_L/R_S$  providing  $R_L > R_S$ .

$$Y_{ins} = \text{Re}(Y_{ins}) + j\text{Im}(Y_{ins}), \quad (7)$$

where

$$\text{Re}(Y_{ins}) = Y_2 \frac{\alpha_1 \alpha_3 + \alpha_2 \alpha_4}{\alpha_3^2 + \alpha_4^2} \quad (8a)$$

$$\text{Im}(Y_{ins}) = Y_2 \frac{\alpha_2 \alpha_3 - \alpha_1 \alpha_4}{\alpha_3^2 + \alpha_4^2} \quad (8b)$$

$$\alpha_1 = \frac{1}{rR_L} (Y_s - Y_2 \tan\theta_2 \tan\theta_s) \quad (8c)$$

$$\alpha_2 = Y_s (Y_s \tan\theta_s + Y_2 \tan\theta_2) \quad (8d)$$

$$\alpha_3 = Y_s Y_2 - Y_s^2 \tan\theta_s \tan\theta_2 \quad (8e)$$

$$\alpha_4 = \frac{1}{rR_L} (Y_2 \tan\theta_s + Y_s \tan\theta_2). \quad (8f)$$

The electrical length  $\theta_S$  of source connecting TL that can transform  $R_S$  to another real impedance at  $f_0$  looking at the first  $J$ -inverter, can be derived as (9) by equating (8b) to zero.

$$\theta_s = \tan^{-1} \left( \frac{-\alpha_6 \pm \sqrt{\alpha_6^2 - 4\alpha_5 \alpha_7}}{2\alpha_5} \right), \quad (9)$$

where

$$\alpha_5 = (R_L^2 Y_2^2 / r^2 - Y_s^4) \tan\theta_2 \quad (10a)$$

$$\alpha_6 = Y_2 Y_s (Y_s^2 - R_L^2 / r^2) (1 - \tan^2\theta_2) \quad (10b)$$

$$\alpha_7 = Y_s^2 (Y_2^2 - R_L^2 / r^2) \tan\theta_2. \quad (10c)$$

Once  $\theta_S$  is calculated, the value of  $\text{Re}(Y_{inS})$  looking at first  $J$ -inverter is determined as (8a). Similarly, using Figure 1B, input admittances ( $Y_{inL}$ ) at last  $J$ -inverter looking toward load terminated impedance ( $R_L$ ) is given as (11).

$$Y_{inL} = \text{Re}(Y_{inL}) + j\text{Im}(Y_{inL}), \quad (11)$$

where

$$\text{Re}(Y_{inL}) = Y_2 \frac{k_1 k_3 + k_2 k_4}{k_3^2 + k_4^2} \quad (12a)$$

$$\text{Im}(Y_{inL}) = Y_2 \frac{k_2 k_3 - k_1 k_4}{k_3^2 + k_4^2} \quad (12b)$$

$$k_1 = 1/R_L(Y_L - Y_2 \tan\theta_2 \tan\theta_L) \quad (12c)$$

$$k_2 = Y_L(Y_L \tan\theta_L + Y_2 \tan\theta_2) \quad (12d)$$

$$k_3 = Y_L Y_2 - Y_L^2 \tan\theta_L \tan\theta_2 \quad (12e)$$

$$k_4 = 1/R_L(Y_2 \tan\theta_L + Y_L \tan\theta_2). \quad (12f)$$

Electrical length  $\theta_L$  of the load connecting the TL that can transform  $R_L$  to another real impedance at  $f_0$  looking at the last  $J$ -inverter is given as (13) by equating (12b) to zero.

$$\theta_L = \tan^{-1} \left( \frac{-k_6 \pm \sqrt{k_6^2 - 4k_5 k_7}}{2k_5} \right), \quad (13)$$

where

$$k_5 = (Y_2^2/R_L^2 - Y_L^4) \tan\theta_2 \quad (14a)$$

$$k_6 = Y_2 Y_L (Y_L^2 - 1/R_L^2) (1 - \tan^2\theta_2) \quad (14b)$$

$$k_7 = Y_L^2 (Y_2^2 - 1/R_L^2) \tan\theta_2. \quad (14c)$$

Once  $\theta_L$  is obtained, the value of  $\text{Re}(Y_{inL})$  looking at the last  $J$ -inverter is determined by using (12a).

## 2.4 | Implementation of J- and K-inverters

Figure 4A shows the parallel-coupled lines and their equivalent  $J$ -inverter. The even- and odd-mode impedances ( $Z_{0ei}$ ,  $Z_{0oi}$ ) of parallel-coupled lines with arbitrary electrical length  $\theta_2$  and characteristic impedance  $Z_2$  are given as (15) in terms of  $J$ -inverter.

$$Z_{0ei} = Z_2 \frac{1 + J_{i,i+1} Z_2 \csc\theta_2 + J_{i,i+1}^2 Z_2^2}{1 - J_{i,i+1}^2 Z_2^2 \cot^2\theta_2} \quad (15a)$$

$$Z_{0oi} = Z_2 \frac{1 - J_{i,i+1} Z_2 \csc\theta_2 + J_{i,i+1}^2 Z_2^2}{1 - J_{i,i+1}^2 Z_2^2 \cot^2\theta_2} \quad (15b)$$

Figure 4B shows the  $K$ -inverter implementation with T-type TLs. The T-type  $K$ -inverter consists of a series TL with a characteristic impedance of  $Z_1$  and electrical length of  $\theta_a$  and a shunt short-circuited TL with a characteristic impedance of  $Z_k$  and electrical length of  $\theta_k$ . The circuit parameters of the T-type  $K$ -inverter can be derived by equating the  $ABCD$ -parameters of the  $K$ -inverter and T-type TLs and are given as (16).

$$\theta_a = -\tan^{-1}(K_{12}/Z_1) \quad (16a)$$

$$\theta_k = \tan^{-1} \left\{ \frac{K_{12} Z_1^2}{Z_1^2 Z_k - K_{12}^2 Z_k} \right\} \quad (16b)$$

The negative electrical length  $\theta_a$  will be absorbed by resonator electrical length  $\theta_0$ . Therefore, the electrical length of the resonator will be shorter than the original length as shown in Figure 1A.

## 2.5 | Step by step design method

Based on the analytical design equations described in previous sections, the step-by-step design guidelines for the proposed IT with center frequency tunability can be summarized as follows.

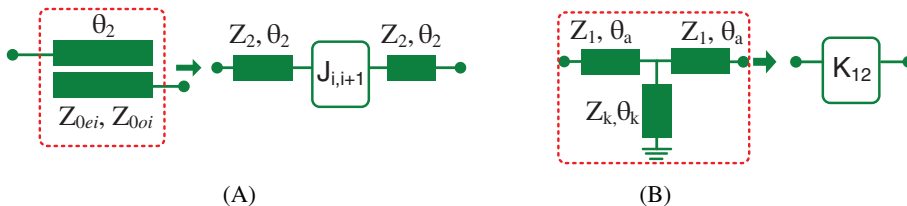


FIGURE 4 Circuit implementation of (A)  $J$ -inverter and (B)  $K$ -inverter

1. The design process starts with setting IT specifications such as the passband ripple,  $\Delta$ ,  $R_S$ ,  $R_L$ .
2. After IT specification is determined, choose resonator parameters such as  $Z_2$ ,  $Z_1$ ,  $\theta_2$ ,  $\theta_1$ ,  $\theta_0$ ,  $C_v$ , and  $f_{ref}$ .
3. Calculate the resonant frequency ( $f_0$ ) by setting  $B = 0$  in (2) or  $X = 0$  in (4). Similarly, calculate the susceptance and react slope parameters  $b$  and  $x$  using (6).
4. Calculate  $\theta_S$  and  $\theta_L$  at  $f_{ref}$  using (9) and (13) by assuming the value of  $Z_S$  and  $Z_L$ , respectively. Once  $\theta_S$  and  $\theta_L$  are obtained, then calculate the values of  $\text{Re}(Y_{ins})$  and  $\text{Re}(Y_{inL})$  from (8b) and (12b), respectively.
5. Calculate the  $J$  and  $K$ -inverter values using (1). After obtaining  $J$ -inverter values, calculate the even- and odd-mode impedances of the parallel-coupled line using (15). For practical implementation of the

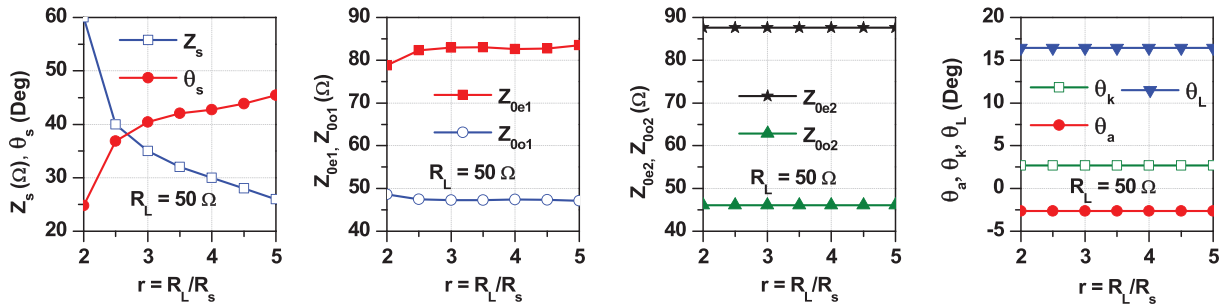


FIGURE 5 Calculated circuit parameters of proposed impedance transformer with  $R_L = 50 \Omega$ ,  $\Delta = 5\%$ , Chebyshev passband ripple of 0.043 dB,  $f_{ref} = 1.5$  GHz,  $C_v = 3$  pF,  $Z_1 = Z_k = Z_L = 70 \Omega$ ,  $Z_2 = 60 \Omega$ ,  $\theta_0 = 12^\circ$ ,  $\theta_1 = 20^\circ$ ,  $\theta_2 = 29.4^\circ$

FIGURE 6 Simulation results of the proposed impedance transformer with tunable center frequency: (A)  $r = 2$  and (B)  $r = 3$

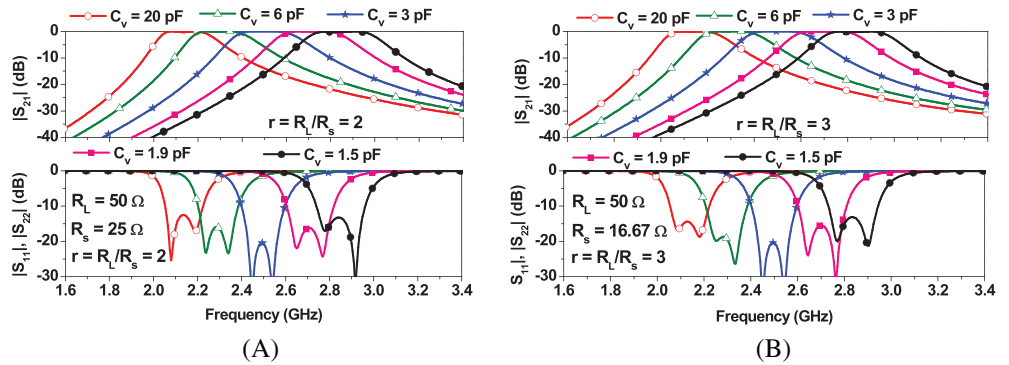


TABLE 1 Calculated circuit parameters

$R_L = 50 \Omega$ ,  $\Delta = 5\%$ , Chebyshev passband ripple = 0.043 dB,  $f_{ref} = 1.5$  GHz,  $C_v = 3$  pF,  $Z_1 = Z_k = Z_L = 70 \Omega$ ,  $Z_2 = 60 \Omega$ ,  $\theta_0 = 12^\circ$ ,  $\theta_1 = 20^\circ$ ,  $\theta_2 = 29.4^\circ$ ,  $\theta_k = 2.67^\circ$ ,  $\theta_a = -2.65^\circ$ ,  $\theta_L = 16.45^\circ$ ,  $Z_{0e2} = 87.63 \Omega$ ,  $Z_{0o2} = 46.08 \Omega$

$r = R_L/R_S$	$Z_S (\Omega)$	$\theta_0 (^\circ)$	$Z_{0e1} (\Omega)$	$Z_{0o1} (\Omega)$	$C_v (\text{pF})$
2	60	24.81	78.77	48.61	1.5 ~ 20
3	35	40.43	82.97	47.27	1.5 ~ 20

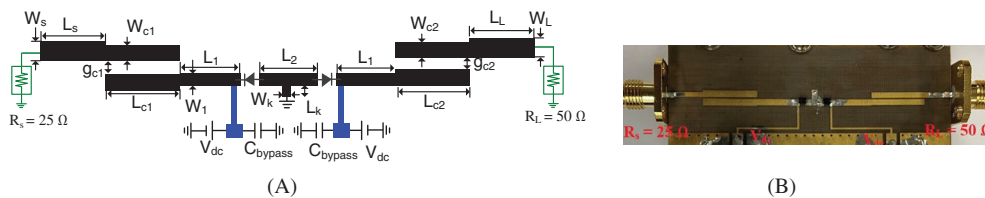


FIGURE 7 (A) Physical layout and (B) photograph of fabricated impedance transformer. Physical dimensions:  $W_s = 1.2$ ,  $W_L = 1.06$ ,  $W_{c1} = 1.28$ ,  $W_1 = W_k = 1.36$ ,  $W_{c2} = 1.50$ ,  $L_s = 5.8$ ,  $L_{c1} = L_{c2} = 12$ ,  $L_1 = 9.5$ ,  $L_2 = 4.36$ ,  $L_k = 2.04$ ,  $L_L = 7.50$ ,  $g_{c1} = 0.18$ ,  $g_{c2} = 0.3$ . Unit: millimeter

$K$ -inverter, calculate  $\theta_a$  and  $\theta_k$  using (16). The negative electrical length  $\theta_{ai}$  will be compensated within  $\theta_0$ , with the result that  $\theta_0$  is shorter than the original value.

- Once all the circuit parameters are determined, the center frequency is tuned by changing the value of  $C_v$ .

Using the step-by-step design guidelines described above, the calculated circuit parameters of the proposed IT are shown in Figure 5. As seen in this figure,  $Z_S$  decreases and  $\theta_S$  increases as the impedance-transforming ratio ( $r$ ) increases. Similarly,  $Z_{0e1}$  slightly increases but  $Z_{0o1}$

decreases as  $r$  increases. However,  $Z_{0e2}$  and  $Z_{0o2}$  remain the same for all  $r$ .

## 2.6 | Design examples

To validate the analytical analysis, Figure 6 shows the frequency response of IT with  $r = 2$  and 3. The circuit parameters are shown in Table 1. These results show that the proposed IT can provide the bandpass filtering response. Besides, the center frequency of IT can be tuned from 2.13 to 2.86 GHz by adjusting capacitance from 20 to 1.5 pF, respectively. These results also confirm that the proposed circuit can integrate IT and the center-frequency tunable bandpass filter within a single device, which is essential for future wireless communication system miniaturization.

## 3 | SIMULATION AND MEASUREMENT RESULTS

For experimental validation, a 25-to-50  $\Omega$  ( $R_S = 25 \Omega$  and  $R_L = 50 \Omega$  with  $r = 2$ ) IT was designed, fabricated, and measured with Chebyshev passband ripple of 0.043 dB,  $\Delta = 5\%$  and  $f_{ref} = 1.5$  GHz on Taconic substrate with a dielectric constant of 2.2 and thickness of 0.787 mm. The calculated circuit parameters are given as  $C_v = 3$  pF,  $Z_S = 60 \Omega$ ,  $Z_L = Z_1 = Z_k = 70 \Omega$ ,  $Z_{0e1} = 78.77 \Omega$ ,  $Z_{0o1} = 48.61 \Omega$ ,  $Z_{0e2} = 87.63 \Omega$ ,  $Z_{0o2} = 46.08 \Omega$ ,  $\theta_2 = 29.4^\circ$ ,  $\theta_1 = 20^\circ$ ,  $\theta_0 = 12^\circ$ ,  $\theta_S = 24.8^\circ$ ,  $\theta_L = 16.45^\circ$ ,  $\theta_a = -1.64^\circ$ , and  $\theta_k = 2.67^\circ$ . The electrical lengths of TL are defined at  $f_{ref} = 1.5$  GHz. The skyworks SMV-1233 varactors are used in this work, which can provide capacitance of 0.9 pF to 20 pF by varying DC bias voltage from 15 to 0 V. Figure 7 shows the physical layout and photograph of fabricated circuit.

Figure 8 shows the simulation and measurement results of fabricated IT. The measured results are consistent with

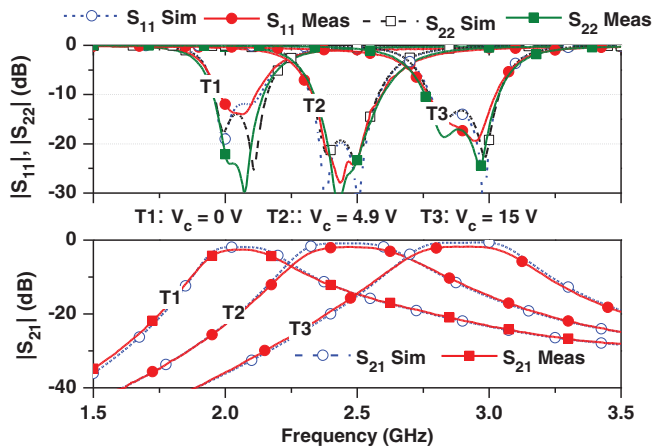


FIGURE 8 Simulation and measurement results of 25-to-50  $\Omega$  ( $r = 2$ ) impedance transformer with tunable center frequency

TABLE 2 Measurement results

$V_{dc}$ (V)	$f_0$ (GHz)	IL (dB)	RL (dB)	3-dB BW (MHz)
15	2.91	1.76	17.2	400
8	2.45	1.88	24.2	400
0	2.05	2.57	13.5	290

Frequency (GHz)	IL (dB)	RL <sub>min</sub> (dB)	$r = R_L/R_S$	A	
8	1.0	0.45	NA	2	No
10	1.0	0.82	20	2	No
11–15	2.60	<1	20	10/2/5	No
16	1	0.60	26	5	No
17	2	NA	18	2	No
18	1	NA	20	5	No
19	2.40	0.72	24.35	10	No
20	3.50	0.72	24.97	25	No
21	2.50	0.88	NA	20	No
This work	2.05 ~ 2.91	2.57 ~ 1.76	13 ~ 18	2	Yes

TABLE 3 Comparison between this work and other state-of-arts

Note: A: Center frequency tunability, RL<sub>min</sub>: Minimum input/output return losses.

simulated results. The measurement results are summarized in Table 2. These results show that the center frequency of IT can be tuned from 2.05 to 2.91 GHz (860 MHz or 34.68% FTR) with insertion loss variation of 2.57 to 1.76 dB by controlling DC bias voltage of 0 to 15 V. The measured 3-dB insertion loss bandwidth varies from 290 to 400 MHz. In addition, the measured input/output return losses are higher than 14 dB within the overall frequency tuning range.

The performance comparison of the proposed IT with previously reported works is shown in Table 3. As observed from this table, the proposed IT provides bandpass filtering response as well as center-frequency tunability capability, which was not possible in previously reported works.<sup>8-23</sup>

## 4 | CONCLUSION

This article demonstrated impedance transformer with tunable center frequency based on filter synthesis approach by using quarter-wave transmission-line resonators. Both analytical analyses and experimental results are shown for validation. For experimental demonstration, a prototype of a 25-to-50  $\Omega$  impedance transformer is designed and fabricated. The fabricated impedance transformer provides not only a wide range of center-frequency tunability but also arbitrary impedance-transforming characteristics. The proposed method can be easily extended to design a higher-order filtering impedance transformer. Therefore, the proposed circuit can integrate the impedance transformer and tunable filter within a single device and play an important role in the circuit miniaturization of next-generation microwave communication systems.

## ACKNOWLEDGMENTS

This work was supported by National Research Foundation of Korea (NRF) grant funded by the Korean government (MSIT) under grant no. 2020R1A2C2012057, in part by the Basic Science Research Program through NRF funded by Ministry of Education under grant no. 2019R1A6A1A09031717, and in part by "Research Base Construction Fund Support Program" funded by Jeonbuk National University 2021.

## DATA AVAILABILITY STATEMENT

The data that support the findings of this study are available on request from the corresponding author. The data are not publicly available due to privacy or ethical restrictions.

## ORCID

Girdhari Chaudhary  <https://orcid.org/0000-0003-2060-9860>

Yongchae Jeong  <https://orcid.org/0000-0001-8778-5776>

## REFERENCES

1. Drozd JM, Joines WT. Using parallel resonators to create improved maximally flat quarter-wavelength transformer impedance matching networks. *IEEE Trans Microw Theory Techn.* 1999;47(2):132-141.
2. Kaymaksut E, François B, Reynaert P. Analysis and optimization of transformer-based power combining for back-off efficiency enhancement. *IEEE Trans Circuits Syst I Regul Pap.* 2013;60(4):825-835.
3. Zito D, Fonte A. Dual-input pseudo-switch RF low noise amplifier. *IEEE Trans Circuits Syst II: Express Br.* 2010;57(9):661-665.
4. Rayno J, Celik N, Iskander MF. Dual-polarization cylindrical long-slot array (CLSA) antenna integrated with compact broadband baluns and slot impedance transformers. *IEEE Antennas Wirel Propag Lett.* 2013;12:1384-1387.
5. Firrao EL, Annema A-J, Nauta B. An automatic antenna tuning system using only RF signal amplitudes. *IEEE Trans Circuits Syst II: Express Br.* 2008;55(9):833-837.
6. Huang Y, Shinohara N, Mitani T. Impedance matching in wireless power transfer. *IEEE Trans Microw Theory Techn.* 2017; 65(2):582-590.
7. Pepe D, Chlis I, Zito D. Transformer-based input integrated matching in cascode amplifiers: analytical proofs. *IEEE Trans Circuits Syst I Regul Pap.* 2018;65(5):1495-1504.
8. Wu Q, Zhu L. Synthesis design of a wideband impedance transformer consisting of two-section coupled lines. *IET Microw Antennas Propag.* 2016;11(1):144-150.
9. Jensen T, Zhurbenko V, Krozer V, Meincke P. Coupled transmission lines as impedance transformer. *IEEE Trans Microw Theory Techn.* 2007;55(12):2957-2965.
10. Chen S, Zhao G, Tang M, Yu Y. Wideband filtering impedance transformer based on transversal interaction concept. *Electron Lett.* 2018;54(6):368-370.
11. Kim P, Chaudhary G, Jeong Y. Ultra-high transforming ratio coupled line impedance transformer with bandpass response. *IEEE Microw Wirel Compon Lett.* 2015;25(7):445-447.
12. Kim P, Chaudhary G, Jeong Y. Wideband impedance transformer with out-of-band suppression characteristics. *Microw Opt Technol Lett.* 2014;56(11):2612-2616.
13. Kim P, Park J, Jeong J, Jeong S, Chaudhary G, Jeong Y. High selectivity coupled line impedance transformer with second harmonic suppression. *J Electromagn Eng Sci.* 2016;16(1):13-18.
14. Kim P, Chaudhary G, Jeong Y. Enhancement impedance transforming ratios of coupled line impedance transformer with wide out-of-band suppression characteristics. *Microw Opt Technol Lett.* 2015;57(7):1600-1603.
15. Kim P, Chaudhary G, Jeong Y. Impedance matching bandpass filter with a controllable spurious frequency based on  $\lambda/2$  stepped impedance resonator. *IET Microw Antennas Propag.* 2018;12(12):1993-2000.
16. Chen M-G, Hou T-B, Tang C-W. Design of planar complex impedance transformers with the modified coupled line. *IEEE Trans Compon Packag Manuf Technol.* 2012;2(10):1704-1710.
17. Wu QS, Zhu L. Wideband impedance transformers on parallel-coupled and multi-section microstrip lines: synthesis design and implementation. *IEEE Trans Compon Packag Manuf Technol.* 2016;6(12):1873-1880.
18. Zhuang Z, Wu Y, Kong M, Wang W. High-selectivity single-ended/balanced DC-block filtering impedance transformer and

- its application on power amplifier. *IEEE Trans Circuits Syst I Regul Pap.* 2020;67(12):4360-4369.
19. Zhu H, Cheong P, Ho SK, Tam KW, Choi W. Realization of extremely high and low impedance transforming ratios using cross-shaped impedance transformer. *IEEE Trans Circuits Syst II: Express Br.* 2020;67(7):1189-1193.
  20. Jeong Y, Chaudhary G, Kim P. Frequency selective impedance transformer with high-impedance transforming ratio and extremely high/low termination impedances. *IEEE Trans Circuits Syst I Regul Pap.* 2021;68(6):2382-2391.
  21. Hsieh C, Lin S, Li J. Bandpass impedance transformers with extremely high transforming ratios using  $\pi$ -tapped feeds. *IEEE Access.* 2018;6:28193-28202.
  22. Roy SCD. Characteristics of single- and multiple-frequency impedance matching networks. *IEEE Trans Circuits Syst II: Express Br.* 2015;62(3):222-225.
  23. Chen W, Wu Y, Wang W, Xu K, Shi J. Synthesis design on wideband single-ended and differential dual-band filtering impedance transformer. *IEEE Trans Circuits Syst II: Express Br.* 2021;68(3):913-916.
  24. N. D. Malyutin, A. V. Andreev, G. A. Malyutin, and R. M. Sharabudinov, Tunable impedance transformer based on split strip lines. *Proceedings of the International Serbian Confer Control and Communications (SIBCON)*, pp. 1–3, 2019.
  25. Kim P, Jeong Y. A new synthesis and design approach of a complex termination impedance bandpass filter. *IEEE Trans Microw Theory Techn.* 2019;67(6):2346-2354.

**How to cite this article:** Chaudhary G, Jeong Y. A design of impedance transformer with tunable center frequencies using filter synthesis approach. *Int J RF Microw Comput Aided Eng.* 2022;e23202. doi:[10.1002/mmce.23202](https://doi.org/10.1002/mmce.23202)